



# Structural characterization and properties of YCrO<sub>3</sub> nanoparticles prepared by reverse micellar method

TOKEER AHMAD<sup>1,\*</sup> and IRFAN H LONE<sup>1,2</sup>

<sup>1</sup>Nanochemistry Laboratory, Department of Chemistry, Jamia Millia Islamia, New Delhi 110025, India

<sup>2</sup>Department of Chemistry, College of Science Yanbu, Taibah University, Almadinah 30002, Saudi Arabia

\*Author for correspondence (tahmad3@jmi.ac.in)

MS received 22 April 2017; accepted 14 June 2017; published online 5 February 2018

**Abstract.** YCrO<sub>3</sub> nanoparticles were prepared by reverse micellar method by the use of surfactant tergitol after heating the precursor sample at 800°C. As-prepared YCrO<sub>3</sub> nanoparticles were characterized by various sophisticated techniques like X-ray diffraction (XRD), transmission electron microscope, Brunauer–Emmett–Teller surface area analyzer, high frequency LCR-meter, superconducting quantum interface device magnetometer and P–E loop tracer. Powder XRD study reveals the formation of highly crystalline orthorhombic monophasic YCrO<sub>3</sub> nanoparticles. The average grain size of as-prepared nanoparticles was found to be 35 nm with the surface area of 348 m<sup>2</sup> g<sup>-1</sup>. Wedge-shaped hysteresis for ferromagnetism and the room temperature ferroelectricity confirm the multiferroic characteristics in the nanoparticles.

**Keywords.** Nanoparticles; reverse micellar synthesis; rare-earth chromates; ferroelectrics; surface area; multiferroics.

## 1. Introduction

The vast interest was generated towards the substances that could show both kinds of ordering in magnetic and electrical properties not because of their technological purpose, but also possess many potential applications in the chain of possible devices [1–6]. Earliest, it was seen that the existence of magnetic and ferroelectric order was difficult to find in the materials as the metal ion demands partially filled and empty d-orbitals, respectively, and hence, the scarcity of multiferroic materials. Later, the alternative mechanisms like local non-centrosymmetric was the main reason to show the ferroelectric behaviour in rare-earth ferrites and chromates that results in the origin of magnetic and ferroelectric properties and lead to the new types of multiferroic compounds [7–10]. The type of perovskites containing chromium oxides was showing much interest by taking their fundamental use and practical applications. The rare-earth chromites (RCrO<sub>3</sub>) with orthorhombic structure were a point of interest in the case of dielectric and magnetic conversions [11]. In addition to the multiferroic nature, these materials show the semiconductor properties [12] and were involved in photocatalytic water splitting for hydrogen evolution, humidity and gas sensor mechanisms [8,13–15]. This may open a new area, where magnetization and polarization in small-sized grains can be potentially used in small devices for the smart applications. Optical switches and sensors based on magneto-optical properties were made with these materials [16,17]. Fabrication of rare-earth chromates and many other ternary oxide compounds involves various synthesis methods [8,18–25]. Recently, we have reported YCrO<sub>3</sub>

nanoparticles for its enhanced multiferroic properties using polymeric citrate precursor route [26]. We could not find any research paper in the literature for the preparation of YCrO<sub>3</sub> nanoparticles using microemulsion procedure. In the present case, we report the synthesis of YCrO<sub>3</sub> nanoparticles using reverse micelles and characterized by various sophisticated techniques like X-ray diffractogram (XRD), transmission electron microscope (TEM), Brunauer–Emmett–Teller surface area analyzer, high frequency LCR-meter, superconducting quantum interface device magnetometer and P–E loop tracer.

## 2. Experimental

High grade chemicals of 0.1 M solutions of yttrium nitrate, chromium nitrate nonahydrate and di-ammonium oxalate monohydrate, respectively, were used in the synthesis procedure by the use of three different microemulsions. In the procedure, the surfactant tergitol (21 ml), co-surfactant 1-octanol (15.6 ml), organic solvent cyclohexane (180 ml) and 10 ml of water solution containing metal salts of Y<sup>3+</sup> and Cr<sup>3+</sup> ions were the constituents of the two microemulsions. In the third microemulsion, constituents are almost same except the 0.1 M water solution of ammonium oxalate monohydrate, which was used as precipitating agent for the metal ions. The two metal ions (Y<sup>3+</sup>, Cr<sup>3+</sup>) microemulsions were added, stirred and after complete dissolution, the third microemulsion was added and again stirred for 2 h at room temperature. The solvent in the whole mixture was evaporated at 60 ± 5°C and green precipitate was obtained for YCrO<sub>3</sub>

nanoparticles. The product was grinded into fine powder and was then calcined 800°C for 12 h.

The phase purity and crystalline nature was analysed by X-ray diffraction on Bruker D8 advance with wavelength ( $\lambda$ ) 1.54056 Å of Ni-filtered CuK $\alpha$  radiation using scanning rate of 10–80°. Morphology and shape of prepared nanosample were examined by FEI Tecnai G<sup>2</sup> 20 TEM operated at 200 kV and by scanning electron microscope (SEM) equipment operated at 30 kV. Surface area, porosity and pore size were determined by BET analyzer of NOVA 2000e USA. For the electrical studies like dielectric and PE measurements, a 10 mm diameter pellet was prepared by mixing of 100 mg YCrO<sub>3</sub> nanoparticles with 2–3 drops of 5% PVA solution and then the dried powder was then pelletized at a pressure of 5 ton and the sintered pellet was prepared. Dielectric and ferroelectric properties were determined by the use of high frequency LCR meter (6505 P, UK) and M/s Radiant Instruments, USA, model loop tracer. Magnetic property was performed by (MPMS) SQUID magnetometer at  $\pm$  60 kOe.

### 3. Results and discussion

X-ray diffraction studies of YCrO<sub>3</sub> compound calcined at 900°C were carried out in the  $2\theta$  range of 10–70°C as shown in figure 1, which shows a high degree of crystallinity indicated by the appearance of intense reflections. The peaks in the XRD pattern correspond to the orthorhombic structure of YCrO<sub>3</sub> (JCPDS: 25-1078). Figure 2a is the TEM image of YCrO<sub>3</sub> nanoparticles synthesized by the microemulsion system employing tergitol as a surfactant. It can be seen that the particles almost show size uniformity and are nearly spherical in shape. Particles are arranged in specific manner giving Y-shaped structure and may be due to the fact that YCrO<sub>3</sub> nanoparticles are magnetic and have high surface area that allows the grain diffusion. The crystalline particles are distributed in the size range of 20–60 nm with an average grain size of 35 nm. The crystallite size of as-prepared material

was also calculated using X-ray Scherrer's studies, which was found to be 54 nm. The X-ray size was found to be larger than the TEM average grain size of 35 nm because TEM size is generally restricted to the smaller sized particles. The high magnification TEM represented in figure 2b shows well-defined lattice fringes that agree the lattice plane of YCrO<sub>3</sub> nanoparticles. To find out the crystalline nature of the prepared nanoparticles, the selected area diffraction technique (SAED) was employed as shown in figure 2c. Concentric circles in the diffraction pattern can be indexed to the highly crystalline orthorhombic YCrO<sub>3</sub> structure that was reproducible with the XRD plot. The high value of BET surface area of 348 m<sup>2</sup> g<sup>-1</sup> was found and the plot is given in figure 2d.

Magnetic and inverse susceptibilities of YCrO<sub>3</sub> nanoparticles are given in figure 3a. The normal magnetic susceptibility ( $\chi_M$ ) sharply decreases with increase in temperature up to the temperature of 135 K and then, remains practically constant. In the case of inverse molar magnetic susceptibility ( $\chi_M^{-1}$ ), the data value initially increases with slow pace by the perturbation of temperature and later shows sharp jumps at around 135 K and again increases gradually. This indicates both types of interactions (ferromagnetic and antiferromagnetic) were possible in YCrO<sub>3</sub> nanoparticles which are temperature-dependent. The presence of this kind of interaction resembles with canted antiferromagnetic system and cause of this feature was because of nanostructure existence [27]. Since the particles in the nanoregime act like independent mini domains which are fluctuating with respect to temperature and this kind of effect was previously explained by Kodama *et al* [28]. The temperature below which the particles show the ferromagnetic interactions at around 90 K and was lower than the previously reported value (110 K) in the literature and the Neel temperature of this study was 125 K and also found lower ( $T_N = 141$  K) than the earlier studied value [29]. Wedge-shaped hysteresis loop was observed as shown in figure 3b and the saturation of 2.134 emu g<sup>-1</sup>, coercive field of 5423 Oe and lastly, the remanent magnetization of 0.5 emu g<sup>-1</sup> were achieved for the prepared YCrO<sub>3</sub> nanoparticles.

There were two type of interactions found in the prepared YCrO<sub>3</sub> nanoparticles, one is ferromagnetic and simultaneously weak antiferromagnetic, which separately depend on the temperature and this may be due to the imperfect superexchange interactions between Cr<sup>3+</sup> ions [30–32]. The room temperature ferroelectric loops as shown in figure 4 of YCrO<sub>3</sub> nanoparticles were measured at 50 kHz. The PE loop was well saturated and the value of remanent polarization of 0.015  $\mu\text{C cm}^{-2}$ , saturation polarization of 0.054  $\mu\text{C cm}^{-2}$  and coercive field of 0.05 kV cm<sup>-1</sup> were found respectively, at an applied voltage of 300 V, however, the area under the loop decreases by the decrease of applied field. The calculated result that was found in the present case was better as compared to the results that were found in the literature [33]. The pellet of as-prepared sample was sintered under static air at 1000°C for 8 h to increase the density of the sample and also removes the pores of the material. Hence, the ferroelectric property could

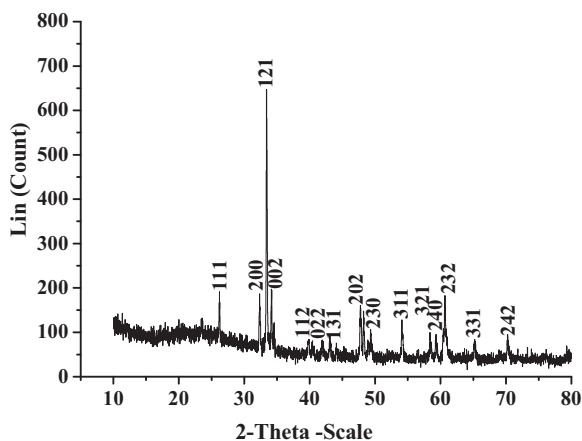


**Figure 1.** PXRD pattern of YCrO<sub>3</sub> nanoparticles.

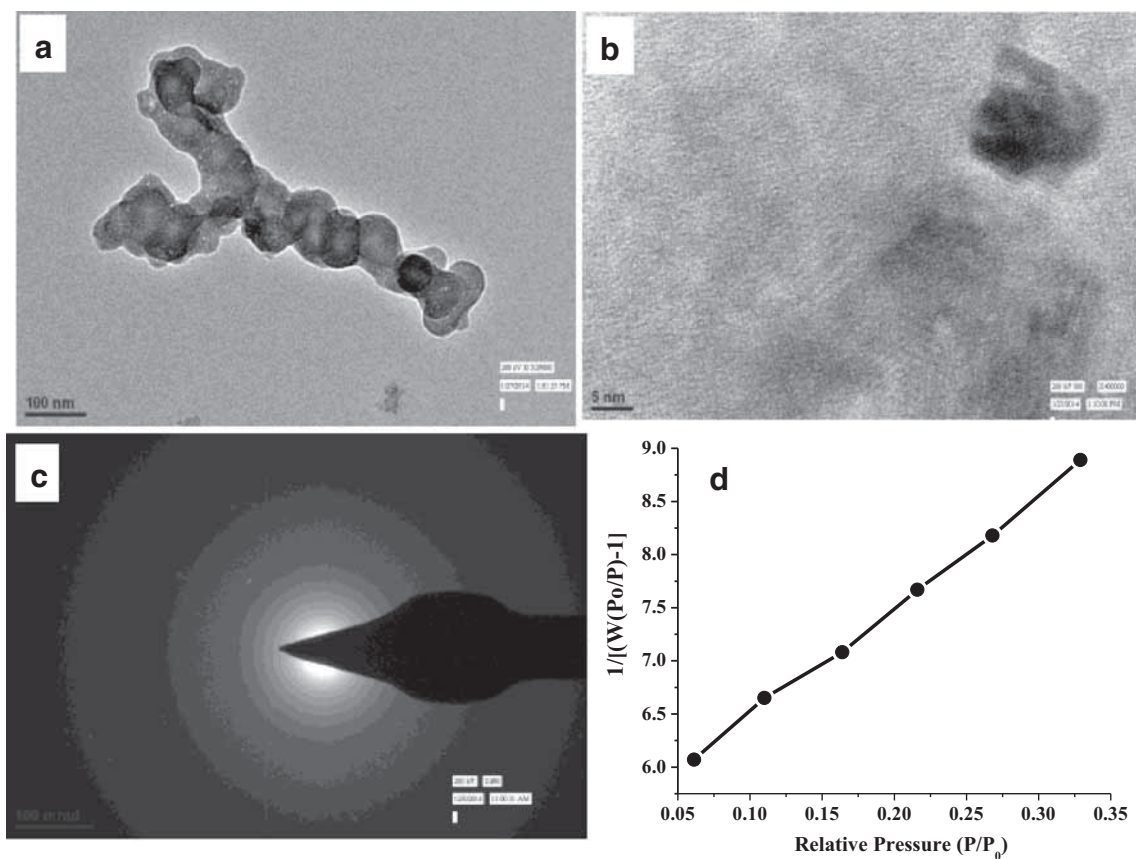


Figure 2. (a) TEM, (b) HR-TEM, (c) SAED images and (d) BET surface area plot of YCrO<sub>3</sub> nanoparticles.

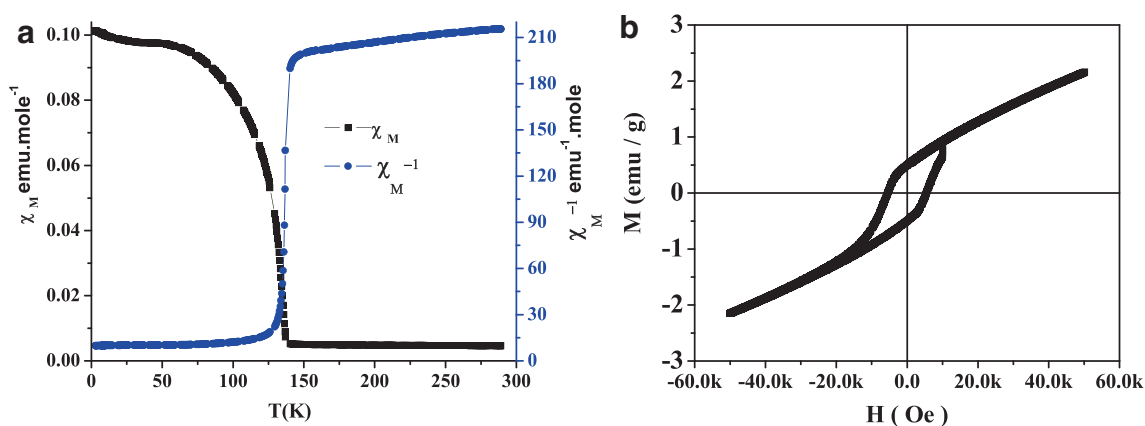
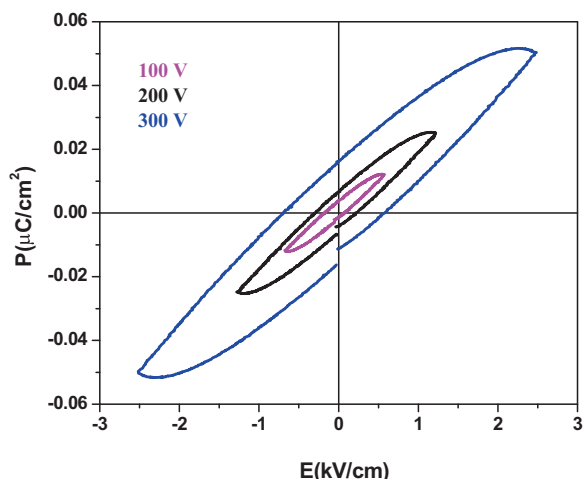


Figure 3. (a) Temperature vs.  $\chi_M$  and  $\chi_M^{-1}$  and (b) ferromagnetic hysteresis loop of YCrO<sub>3</sub> nanoparticles.

originate from the prepared sample and not from the pore capacitance of the material. The origin of ferroelectricity in YCrO<sub>3</sub> nanoparticles was earlier given by Rao *et al* [34], and it was found that the local or neighbouring interaction results in the non-centrosymmetry in YCrO<sub>3</sub> [35]. The variation of dielectric properties with temperature of YCrO<sub>3</sub> nanoparticles at different frequencies between 1 and 2 MHz were studied in the temperature range of 150–400°C as shown in figure 5a

and b. The dielectric values decrease by the rise of the frequency and a kind of anomaly was also found between the temperatures of 275 and 300°C and showed the peak maxima at ~275°C. The dielectric constant goes through a broad maximum similar to the CeCrO<sub>3</sub> compound reported earlier, which may again be similar to the diffuse phase transition as seen in relaxor materials [36]. This kind of dielectric variation was shown with relaxor type of dielectric materials and such



**Figure 4.** Polarization–electric (P–E) loops of YCrO<sub>3</sub> nanoparticles at different applied fields.

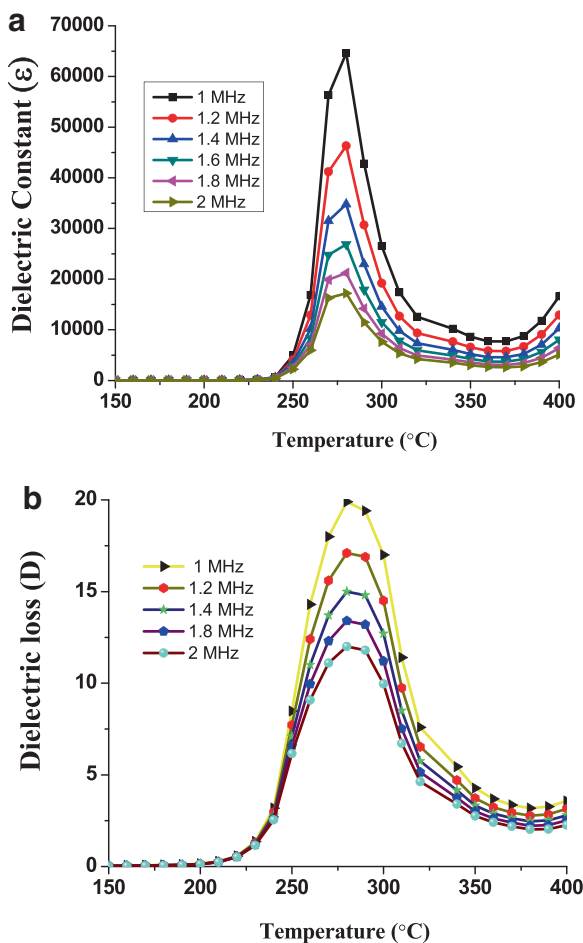


**Figure 5.** Temperature dependence of (a) dielectric constant and (b) dielectric loss of YCrO<sub>3</sub> nanoparticles.

anomaly could be related to ferroelectric phases at that particular temperature and it is dependent on frequencies, which

means that as the frequency increases, the intensity of peak declines [26,37]. Both the dielectric constant and dielectric loss decrease with the increase in frequency. The observed behaviour is expected to be associated to the failure of electric dipoles to follow the pace of change of polarization with respect to the change of applied alternating field [38,39]. A new series of oxides of YCrO<sub>3</sub> can be prepared such as La<sub>1-x</sub>Ce<sub>x</sub>CrO<sub>3</sub> by substituting the dopant of lanthanum ions, which have tunable band gap wherein its absorption shifts from UV to visible light and may have potential importance in magnetic and electric properties [40].

#### 4. Conclusion

In summary, monophasic and nanocrystalline YCrO<sub>3</sub> (35 nm) was prepared by reverse micellar method using tergitol as the surfactant. The structural characterization and detailed analysis of the surface area and dielectric properties were studied for the as-prepared YCrO<sub>3</sub> nanoparticles. Multiferroic nature of YCrO<sub>3</sub> nanoparticles was established by ferromagnetic and room temperature ferroelectric studies with significant data values. The combining properties such as ferromagnetic, ferroelectric and dielectric functionalities of YCrO<sub>3</sub> nanoparticles make it applicable in electronic and magnetic devices.

#### Acknowledgements

We thank DST and Jamia Millia Islamia, New Delhi, India, for financial support. We also thank Prof K V Ramanujachary (Rowan University, USA), for carrying out magnetic measurements, and AIIMS, New Delhi, for electron microscopic studies. For the P–E study, we must thank Dr V R Reddy, UGC-DAE, Indore, and IHL thanks UGC, New Delhi, for senior research fellowship.

#### References

- [1] Hill N A 2000 *J. Phys. Chem. B* **104** 6694
- [2] Fiebig M 2005 *J. Phys. D* **38** 123
- [3] Prellier W, Singh MP and Murugavel P 2005 *J. Phys.: Condens. Matter* **17** 803
- [4] Eerenstein W, Mathur N D and Scott J F 2006 *Nature* **442** 759
- [5] Cheong S W and Mostovoy M 2007 *Nat. Mater.* **6** 13
- [6] Ramesh R and Spaldin N A 2007 *Nat. Mater.* **6** 21
- [7] Sahu J R, Serrao C R, Ray N, Waghmare U V and Rao C N R 2007 *J. Mater. Chem.* **17** 42
- [8] Ahmad T, Lone I H, Ansari S G, Ahmed J, Ahamad T and Alshehri S M 2017 *Mater. Des.* **126** 331
- [9] Su Y L, Zhang J C, Li L, Feng Z J, Li B Z, Zhou Y *et al* 2010 *Ferroelectrics* **410** 102
- [10] Jaiswal A, Das R, Vivekanand K, Maity T, Abraham P M, Adyanthaya S *et al* 2010 *J. Appl. Phys.* **107** 013912

- [11] Rao G V S, Wanklyn B M and Rao C N R 1971 *J. Phys. Chem. Solids* **32** 345
- [12] Tsushima K, Aoyagi K and Sugano S 1970 *J. Appl. Phys.* **41** 1238
- [13] Lakshmi D and Sundaram R 2008 *Sens. Transducers J.* **97** 74
- [14] Siemons M and Simon U 2007 *Sens. Actuators B* **126** 181
- [15] Fergus J W 2004 *Solid State Ionics* **171** 1
- [16] Didosyan Y S, Hauser H, Reider G A and Toriser W 2004 *J. Appl. Phys.* **95** 7339
- [17] Didosyan Y S, Hauser H and Nicolics J 2000 *Sens. Actuators A: Phys.* **81** 263
- [18] Ahmad T, Khatoon S and Coolahan K 2013 *Mater. Res. Bull.* **48** 3065
- [19] Thakur J, Shukla R, Raje N, Ghonge D, Bagla H and Tyagi A K 2011 *Nanosci. Nanotechnol. Lett.* **3** 648
- [20] Ganguli A K, Vaidya S and Ahmad T 2008 *Bull. Mater. Sci.* **31** 415
- [21] Ahmad T and Ganguli A K 2006 *Mater. Lett.* **60** 3660
- [22] Duran A, Arevalo-Lopez A M, Castillo-Martinez E, Guaderama M G, Moran E, Cruz M P *et al* 2010 *J. Solid State Chem.* **183** 1863
- [23] Ahmad T, Lone I H, Ubaidullah M and Coolhan K 2013 *Mater. Res. Bull.* **48** 4723
- [24] Al-Hartomy O A, Ubaidullah M, Khatoon S, Madani J H and Ahmad T 2012 *J. Mater. Res.* **27** 2479
- [25] Ahmad T, Lone I H and Ubaidullah M 2015 *RSC Adv.* **5** 58065
- [26] Ahmad T and Lone I H 2016 *New J. Chem.* **40** 3216
- [27] Bedekar V, Shukla R and Tyagi A K 2007 *Nanotechnology* **18** 155706
- [28] Kodama R H, Makhlouf S A and Berkowitz A E 1997 *Phys. Rev. Lett.* **79** 1393
- [29] Tiwari B, Surendra M K and Rao M S R 2013 *J. Phys. Condens. Matter* **25** 216004
- [30] Blazey K W and Burns G 1967 *Proc. Phys. Soc. London* **91** 640
- [31] Dzyaloshinsky I 1958 *J. Phys. Chem. Solids* **4** 241
- [32] Moriya T 1960 *Phys. Rev.* **120** 91
- [33] Cheng Z X, Wang X L, Dou S X, Kimura H and Ozawa K 2010 *J. Appl. Phys.* **107** 09D905(1-3)
- [34] Rao C N R and Serrao C R 2007 *J. Mater. Chem.* **17** 4931
- [35] Singh I, Nigam A K, Landfester K, Munoz-Espi R and Chandra A 2013 *Appl. Phys. Lett.* **103** 182902
- [36] Shukla R, Bera A K, Yusuf S M, Deshpande S K, Tyagi A K, Hermes W *et al* 2009 *J. Phys. Chem. C* **113** 12663
- [37] Grover V, Shukla R, Jain D, Deshpande S K, Arya A, Pillai C G S *et al* 2012 *Chem. Mater.* **24** 2186
- [38] Wagner K W 1913 *Ann. Phys.* **40** 817
- [39] Koops C G 1951 *Phys. Rev.* **83** 121
- [40] Shukla R, Manjanna J, Bera A K, Yusuf S M and Tyagi A K 2009 *Inorg. Chem.* **48** 11691